ELSEVIER

Journal of Molecular Catalysis A: Chemical 182–183 (2002) 35–46

JOURNAL OF MOLECULAR CATALYSIS A: CHEMICAL

www.elsevier.com/locate/molcata

Microemulsion-assisted synthesis of catalysts based on aluminium and magnesium phosphates

María Ángeles Aramendía, Victoriano Borau, César Jiménez*, José María Marinas, Francisco José Romero[1], Francisco José Urbano

Department of Organic Chemistry, University of Córdoba, Campus de Rabanales, Edificio C-3, Ctra. Nnal. IV-A, KM 396, E-14014 Córdoba, Spain

Received 2 July 2001; accepted 31 October 2001

Abstract

Various materials consisting of magnesium (mMgPO-1 and mMgPO-2) or aluminium phosphates (mAlPO-1 and mAlPO-2) were synthesized from microemulsions and characterized in structural terms using X-ray diffraction (XRD), energy dispersive X-ray analysis (EDAX), thermal analysis, and solid-state ^{31}P and ^{27}Al NMR spectroscopies. The morphology of the solids was examined by scanning electron microscopy (SEM) and transmission electron microscopy (TEM), and their surfaces properties were determined from N_2 adsorption–desorption isotherms. The new materials thus prepared are structurally and compositionally similar to solids obtained by precipitation from solutions; their specific surface areas, however, are substantially greater and their pore size distribution more narrow. The catalytic activity of the materials in the dehydration–dehydrogenation of isopropyl alcohol was found to be similar to or greater than that of catalysts obtained by precipitation from aqueous solutions. The magnesium orthophosphates yielded acetone (the major product) and propene from 2-propanol; the aluminium orthophosphates, which possess dehydrating activity only, yielded propene alone.

Keywords: Microemulsions; Magnesium phosphates; Aluminium phosphates; Heterogeneous catalysis; Isopropyl alcohol

1. Introduction

The preparation of new solid materials for use as catalysts, sorbents, semiconductors or products with magnetic or optical properties entails increasingly stricter control of the synthetic procedure. Some of the many procedures available for this purpose use auxiliary organic molecules as templates. Thus, zeolites and various other molecular sieves are frequently obtained by using small organic molecules for this purpose [1]. One alternative approach involves using more organized systems as templates; such is the case with surfactants such as those in the M41S molecular sieve family, which self-assemble into spherical or rod-like micelles in aqueous solutions [2]. While pore size in zeolites falls in the molecular range (0.3–1.2 nm), that in M41S sieves lies in the mesopore range (2–10 nm).

One other alternative is the use of water-in-oil (w/o) microemulsions, which are thermodynamically stable isotropic dispersions of an aqueous phase

* Corresponding author. Tel.: +349-57-218-638; fax: +349-57-212-066.
E-mail addresses: qo1jisac@uco.es (C. Jiménez), qo2rosaf@uco.es (F.J. Romero).
[1] Co-corresponding author. Tel.: +349-57-212-065; fax: +349-57-212-066.

1381-1169/02/$ – see front matter
PII: S1381-1169(01)00470-8

in a continuous oil phase [3]. Water confined in the reversed micelles thus formed can be used as a reaction medium to synthesize nanoparticles; the small size of the aqueous droplets restricts particle growth and ensures a narrow size distribution. Precipitation reactions can be implemented by having the contents of the aqueous droplets exchanged via collision and coalescence between micelles. This procedure has been used to obtain nanoparticles of various types of materials including silver halides for photographic emulsions, magnetic substances and superconductors [3]. A sizeable fraction of research in this field has focused on the synthesis of metal nanoparticles [4,5] such as those of metal-supported catalysts obtained from microemulsions and used in processes such as CO hydrogenation [6], CO_2 hydrogenation [7] or methanol production from syngas [8], as well as Al_2O_3-supported CeO_2/ZrO_2 solids for the oxidation of CO [9]; the former solids have proved more active than catalysts prepared by impregnation and the latter more than those obtained by precipitation.

Solids containing magnesium orthophosphates and aluminium orthophosphates have been used as catalysts for a variety of organic processes [10,11]. Thus, magnesium orthophosphates have been employed in the transformation of alcohols [12], the Meerwein–Ponndorf–Verley–Oppenauer reaction [14], vapour-phase aldol condensations [13], the *N*-alkylation of aniline with methanol [15], the oxidative dehydrogenation of ethane and the oxidative coupling of methane [16,17]. Aluminium orthophosphates have be used as catalysts in the dehydration of alcohols [18], alkylation reactions [19], condensation reactions [20] and cracking processes [21], among others.

In this work, we used microemulsions to prepare various aluminium and magnesium orthophosphates that were subsequently characterized and used as catalysts in the dehydration/dehydrogenation of isopropyl alcohol.

2. Experimental

The surfactant used to prepare the microemulsions was Triton N-101 (polyethylene glycol nonylphenyl ether) and purchased from Aldrich. Before any solid was synthesized, the concentration range over which the water/surfactant/cyclohexane emulsions remained stable was determined.

2.1. Synthetic procedure

Solid mAlPO-1 was obtained from two microemulsions (A and B). Microemulsion A was prepared by mixing 100 g of a solution containing 0.5. M Triton N-101 in cyclohexane with 5 g of another containing 1 M $Al(NO_3)_3{\cdot}6H_2O$ and 1 M (85%) H_3PO_4 in water. Microemulsion B was obtained by mixing 100 g of a solution of 0.5 M Triton N-101 in cyclohexane with 5 g of another consisting of 3 M (25%) ammonia in water. The microemulsion obtained by mixing A and B, with pH = 9, was stirred for 1 h and allowed to stand for 3 days, after which it was disrupted by adding of 300 ml of acetone. The suspension thus formed was allowed to stand for 3 days, after which the solid was collected by centrifugation and dried in a stove at 105 °C.

Solid mAlPO-2 was obtained by a similar procedure but using half the previous amount of microemulsion A. Solid mMgPO-1 was also prepared from two microemulsions (A and B). Microemulsion A was obtained by mixing 200 g of a solution containing 0.5 M Triton N-101 in cyclohexane with 10 g of another consisting of 1.5 M $Mg(NO_3)_2{\cdot}6H_2O$ and 1 M (85%) H_3PO_4 in water. Microemulsion B was prepared by mixing 200 g of a solution of 0.5 M Triton N-101 in cyclohexane with 10 g of another containing 3 M NaOH in water. This emulsion remained turbid throughout. The emulsion resulting from the mixing of A and B (pH = 8) was stirred for 1 h and allowed to stand for 3 days, after which it was disrupted by addition of 300 ml of acetone and allowed to stand for another 3 days. Finally, the resulting solid was collected by centrifugation and dried in a stove at 105 °C.

Solid mMgPO-2 was prepared similarly to mMgPO-1 but using a mixture of 200 g of 0.5 M Triton N-101 in cyclohexane with 5 g of 1.5 M $Mg(NO_3)_2{\cdot}6H_2O$ and 1 M (85%) H_3PO_4 in water as microemulsion A. The solids were repeatedly washed with about 100 ml of acetone and separated by centrifugation. Finally, all were calcined at 600 °C for 3 h, the heating rate being 5 °C min^{-1}.

2.2. Characterization

X-ray diffraction (XRD) patterns were recorded on a Siemens D 5000 diffractometer using Cu Kα radiation. Scans were performed over the 2θ range from 2 to 80. Thermogravimetric and differential thermal analysis curves were recorded on a Setaram Setsys 12 thermal analysis station by heating in an argon atmosphere from 25 to 1200 °C at a rate of 5 °C min^{-1}.

Solid-state ^{31}P NMR spectra were recorded on a Bruker ACP-400 spectrometer at 161.975 MHz at room temperature. Typical spinning speeds (4 kHz) were used with all samples. The excitation pulse and recycle time were 5 μs ($\pi/2$ pulse) and 5 s (300 scans), respectively. ^{31}P shifts were measured relative to H_3PO_4.

^{1}H MAS NMR spectra were obtained at 400.13 MHz on a Bruker ACP-400 spectrometer at room temperature. An overall 1000 free induction decays were accumulated. The excitation pulse and recycle time were 5 μs and 3 s, respectively. Chemical shifts were measured relative to a tetramethylsilane standard. Prior to measurement, samples were dehydrated in a stove at 150 °C for 24 h.

The composition of the catalysts was determined by energy dispersive X-ray analysis (EDAX) on a Jeol JSM-5400 instrument equipped with a Link ISI analyser and a Pentafet detector (Oxford). Scanning electron microscopy (SEM) was carried out on a JEOL 6300 microscope with an Au-sputtered specimen. Transmission electron microscopy (TEM) was performed on a JEOL 200 CX microscope using copper grids. The specific surface area of each solid was determined by using the BET method on a Micromeritics ASAP 2000 analyser.

Reactions were conducted in a flow-through fixed-bed reactor connected to a gas chromatograph; the reactor was fed at the top with isopropyl alcohol by means of a Sage 351 propulsion pump. The alcohol was transferred to an evaporator where it was mixed with the carrier gas (N_2), which allowed the reactor's feed rate to be adjusted. The reaction products were directly inserted into a gas chromatograph and analysed using a methyl silicone 100 m × 0.25 mm ID fused silica capillary column at a constant temperature (45 °C). No diffusion control mechanism was detected [22], nor was any of the reactor parts found to contribute to the catalytic effect under the working conditions used in preliminary blank runs.

3. Results and discussion

3.1. Powder XRD and EDAX analyses

The XRD patterns for solids mAlPO-1 and mAlPO-2 exhibit a single, broad band at $2\theta = 12$–36 typical of microcrystalline $AlPO_4$ with a highly disperse crystallite size, even after calcination at 600 °C (Fig. 1). These solids are thus less crystalline than those obtained by other authors under similar conditions—which exhibit the bands for the tridymite phase above temperatures around 600 °C [23,24].

On the other hand, solids mMgPO-1 and mMgPO-2 are amorphous after heating in a stove but exhibit diffraction bands upon calcination at 600 °C (Fig. 2). The bands can be assigned to no known magnesium phosphate structure; in any case, the bands for periclase MgO, though weak, are present and increased in strength with further calcining (to 800 °C). There are no bands for farringtonite $Mg_3(PO_4)_2$; in fact, the solid appears to be crystalline above about 650 °C. The absence of these bands was previously noted for other solids obtained from magnesium and phosphate ions precipitated with NaOH [25].

Table 1 shows the elemental composition of the studied solids. Solids mAlPO-1 and mAlPO-2 possess an Al/P ratio of 1.0 and 1.2, respectively, which suggests that both consist of $AlPO_4$—albeit in a different

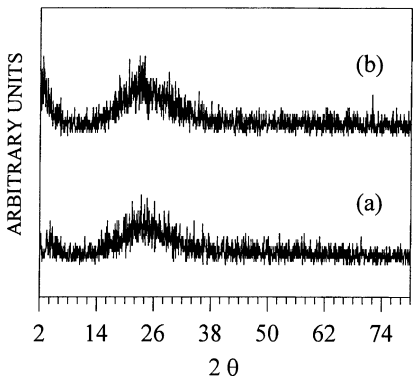

Fig. 1. XRD patterns for solids mAlPO-1 (a) and mAlPO-2 (b) calcined at 600 °C.

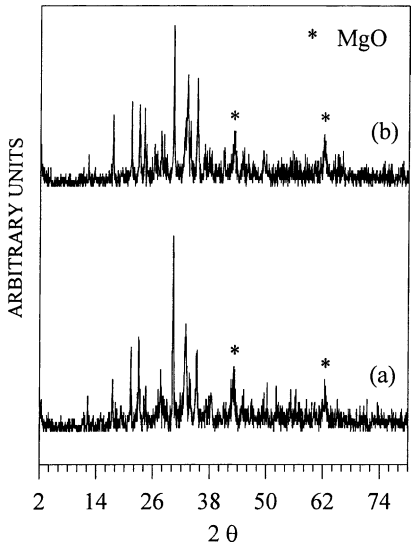

Fig. 2. XRD patterns for solids mMgPO-1 (a) and mMgPO-2 (b) calcined at 600 °C.

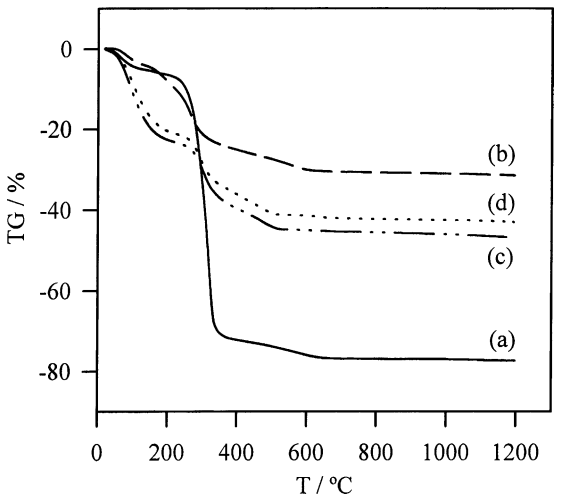

Fig. 3. TGA curves for solids: (a) mAlPO-1; (b) mAlPO-2; (c) mMgPO-1; (d) mMgPO-2.

stoichiometry—no XRD signals for crystalline Al_2O_3 were detected. Solids mMgPO-1 and mMgPO-2 possess an Mg/P ratio of 1.5 and 1.7, respectively. Although the theoretical Mg/P ratio for $Mg_3(PO_4)_2$ is 1.5, this phase was present in none of the solids as it was not detected in the XRD patterns of the samples calcined at 800 °C—which contained periclase instead. Like previously reported solids obtained in a similar manner, both mMgPO-1 and mMgPO-2 contain a high proportion of sodium.

3.2. Thermal analysis

Fig. 3 shows the thermogravimetric curves for the fresh solids. Those for mAlPO-1 and mAlPO-2 exhibit three different steps. Below 100 °C, the solids undergo a rapid weight loss of about 5% corresponding to adsorbed water. Between 150 and 400 °C the solids exhibit a substantial weight loss, which may be related to constitutional water. Above 400 °C a minor weight loss (4 and 6% for mAlPO-1 and mAlPO-2) is observed that corresponds to water formed by condensation of hydroxyl surface groups. These losses may also include surfactant molecules adsorbed on phosphate particles. Note the enormous difference in weight loss over the range 150–400 °C between solids mAlPO-1 and mAlPO-2; the loss is much marked in the former, which must thus be more extensively hydrated than the latter (obtained by using twice more ammonium hydroxide). An increased weight loss in this range has also been associated to a lower Al/P ratio [24].

The thermogravimetric curves for solids mMgPO-1 and mMgPO-2 are very similar. The first weight loss, slightly greater than 20%, takes place at around 90 °C and must be due to crystallization water; it is consistent with previously observed losses in highly hydrated magnesium phosphates present in solids prepared in a similar manner [25]. The second weight loss occurs at around 300 °C and amounts to about 15%, and the third (ca. 5%) above 400 °C. These latter losses must correspond to the release of water (from hydrated phosphates in the former case and from the dehydration of $Mg(OH)_2$ to MgO [26], detected by XRD, in the latter). This range may also be the one where surfactant adsorbed on the solid particles is

Table 1
Elemental composition (at.%) of the solids calcined at 600 °C as determined by EDAX

Solid	Al	Mg	P	O	Na	Cl
mAlPO-1	14.8	–	14.2	69.1	–	1.9
mAlPO-2	14.4	–	12.0	73.6	–	–
mMgPO-1	–	17.8	11.7	60.9	9.6	–
mMgPO-2	–	17.3	10.4	62.3	10.0	–

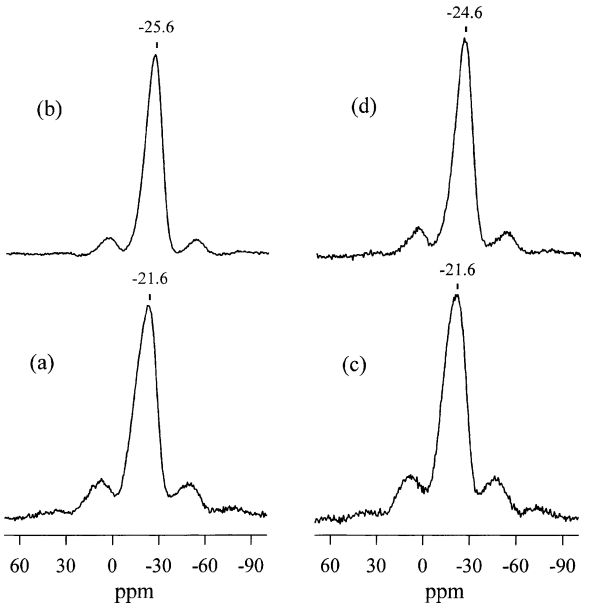

Fig. 4. ^{31}P MAS NMR spectra for solids: (a) mAlPO-1; (b) calcined mAlPO-1; (c) mAlPO-2; (d) calcined mAlPO-2.

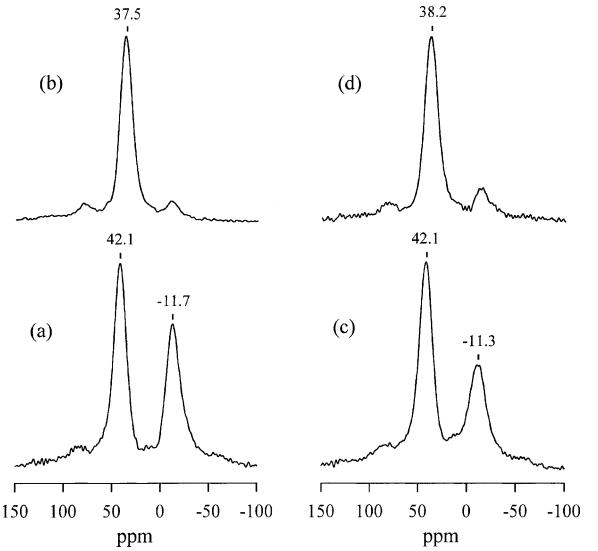

Fig. 5. ^{27}Al MAS NMR spectra for solids: (a) mAlPO-1; (b) calcined mAlPO-1; (c) mAlPO-2; (d) calcined mAlPO-2.

removed. Some such molecules are carbonized; in fact, the solids calcined at 600 °C exhibit a greyish appearance after the thermal treatment. The DTA curve (not shown) also contains an exothermic peak at 522 and 505 °C for mMgPO-1 and mMgPO-2, respectively, which is associated to no weight loss but rather to some phase change or solid-state reaction.

3.3. ^{31}P and ^{27}Al MAS NMR spectroscopy

The ^{31}P MAS NMR spectra for solids mAlPO-1 and mAlPO-2 (Fig. 4) exhibit a single resonance, at ca. −25 ppm, and a series of spinning side bands. This signal corresponds to P atoms in octahedral coordination as parts of $P(OAl)_4$ units [27]. The ^{27}Al MAS NMR spectra for the uncalcined solids exhibit two components at 42 and −11 ppm that correspond to tetrahedral and octahedral aluminium, respectively, in $AlPO_4$ (Fig. 5). The absence of resonance at ca. 7 ppm allows one to discard the presence of γ-Al_2O_3 [27]. The proportion of octahedral aluminium is greater in solid mAlPO-1 than in mAlPO-2, which also consistent with the increased weight loss in the former. Calcination leads to the disappearance of the signal at −11 ppm for mAlPO-1 and also to the virtual disappearance of that for mAlPO-1—no narrowing in the signal for tetrahedral aluminium $[Al(OP)_4]$ is observed, however. Also, relative to solids obtained by precipitation from a conventional solution [27], those obtained from microemulsions exhibit a broader band for tetrahedral aluminium and are thus less crystalline. The ^{1}H spectra (not shown) exhibit a peak at 3.6 ppm corresponding to P–OH groups in addition to smaller signals at 0–1 ppm corresponding to Al–OH groups [27].

The ^{31}P spectra for uncalcined solids mMgPO-1 and mMgPO-2 exhibit a signal at 3.5 ppm and its associated spinning side bands (Fig. 6). In previous work, the $Mg_3(PO_4)_2{\cdot}8H_2O$ phase was found to exhibit a signal at 4.6 ppm [28]. Also, amorphous $Mg_3(PO_4)_2$ was found to exhibit a signal at 0.5 ppm upon calcination—that for the crystalline farringtonite phase obtained above 500 °C appeared at −0.5 ppm. By contrast, calcined mMgPO-1 and mMgPO-2 exhibit two signals at 5.0 and 2.5 ppm. This confirms the XRD results, which provide no evidence of the presence of these phases. Both signals must correspond to new Na-containing phases, as suggested by the composition of the samples. The $NaMgPO_4$ phase, present in other materials previously synthesized by our group, exhibits a chemical shift of 1.8 ppm [29].

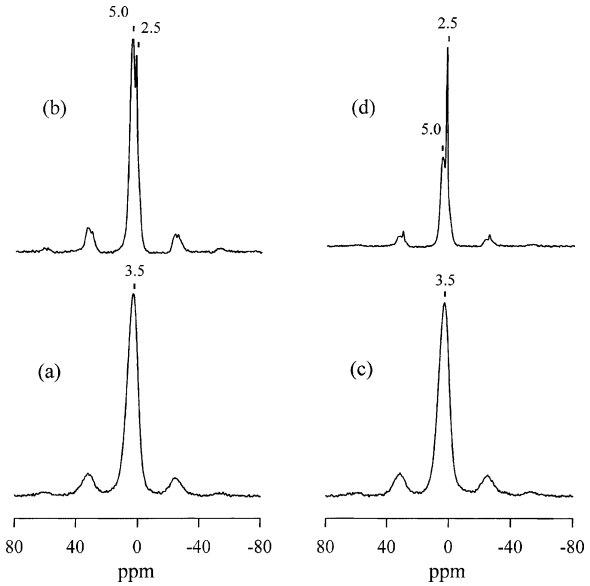

Fig. 6. ^{31}P MAS NMR spectra for solids: (a) mMgPO-1; (b) calcined mMgPO-1; (c) mMgPO-2; (d) calcined mMgPO-2.

3.4. SEM and TEM studies

The scanning electron micrographs for solids mAlPO-1 and mAlPO-2 (Fig. 7) calcined at 600 °C show smooth particles of uneven shape and size. A magnified view of the particles reveals the presence of aggregates. Solids mMgPO-1 and mMgPO-2, when calcined, also consist of smooth particles of uneven shape and size a magnified view of which also reveals that they consist of smaller particles. Calcination alters the morphology of these solids, which consist of larger, more uniform (particularly in mMgPO-2) but less consolidated particles than the previous ones.

Fig. 8 shows selected transmission electron micrographs for solids mMgPO-1 and mMgPO-2. The two are morphologically similar in both calcined and uncalcined form, and consist of aggregates of unevenly shaped and sized particles. Particle size ranges from 30 to 180 nm. The particles contain pores of variable size up to 70 nm that lead to seemingly hollow particles the walls of which contain smaller pores—many are 20 nm in size but some are as small as 5 nm. These particles may have formed by aggregation of smaller particles, the voids in the aggregates making up the meso and macroporous systems of the material.

Solids mAlPO-1 and mAlPO-2 are also highly similar to each other but rather different from mMgPO-1 and mMgPO-2 (Fig. 9). As can be seen, the former exhibit a smaller particle size than the latter. Also, the aluminium phosphates obtained from a microemulsion can be assumed to consist of aggregates of more or less elongated, smaller particles forming a network with many voids. Although similar in appearance, the calcined solids contain larger particles than the uncalcined solids as a result of the high synthesis temperatures used. A magnified view of the particles reveals the presence of a disordered system of mesopores about 7 nm in size.

3.5. Textural properties

Upon calcination, all four solids studied exhibit type IV N_2 adsorption isotherms (Fig. 10), which are typical of mesoporous solids as per the BDDT classification [30]. Table 2 gives the specific surface area, pore volume and average pore diameter of the solids. The aluminium orthophosphates prepared in microemulsions possess a specific surface area of 340 $m^2\,g^{-1}$ for mAlPO-1 and 370 $m^2\,g^{-1}$ for mAlPO-2; both values are much greater than those for similar phosphates obtained by precipitation with ammonia (between 100 and 160 $m^2\,g^{-1}$) and also than those for aluminium orthophosphates gelled in the presence of an organic neutralizing agent such as ethylene oxide or propylene oxide (viz. 257 and 271 $m^2\,g^{-1}$, respectively) [23,31]. Also, our solids exhibit a more narrow pore size distribution, with an average pore diameter of ca. 7–8 nm. These values are similar to those determined by TEM. The N_2 adsorption–desorption isotherms for solids mAlPO-1 and mAlPO-2 exhibit a hysteresis cycle in between those of the H_1 and H_2 types [32,33]. Type H_1 cycles are associated to

Table 2
Specific surface area (S_{BET}), pore volume and pore diameter for the studied phosphates

Solid	S_{BET} ($m^2\,g^{-1}$)	Pore volume ($ml\,g^{-1}$)	BJH pore size (Å)
mAlPO-1	339.5	0.944	79
mAlPO-2	370.9	0.954	70
mMgPO-1	12.6	0.087	262
mMgPO-2	16.1	0.123	302

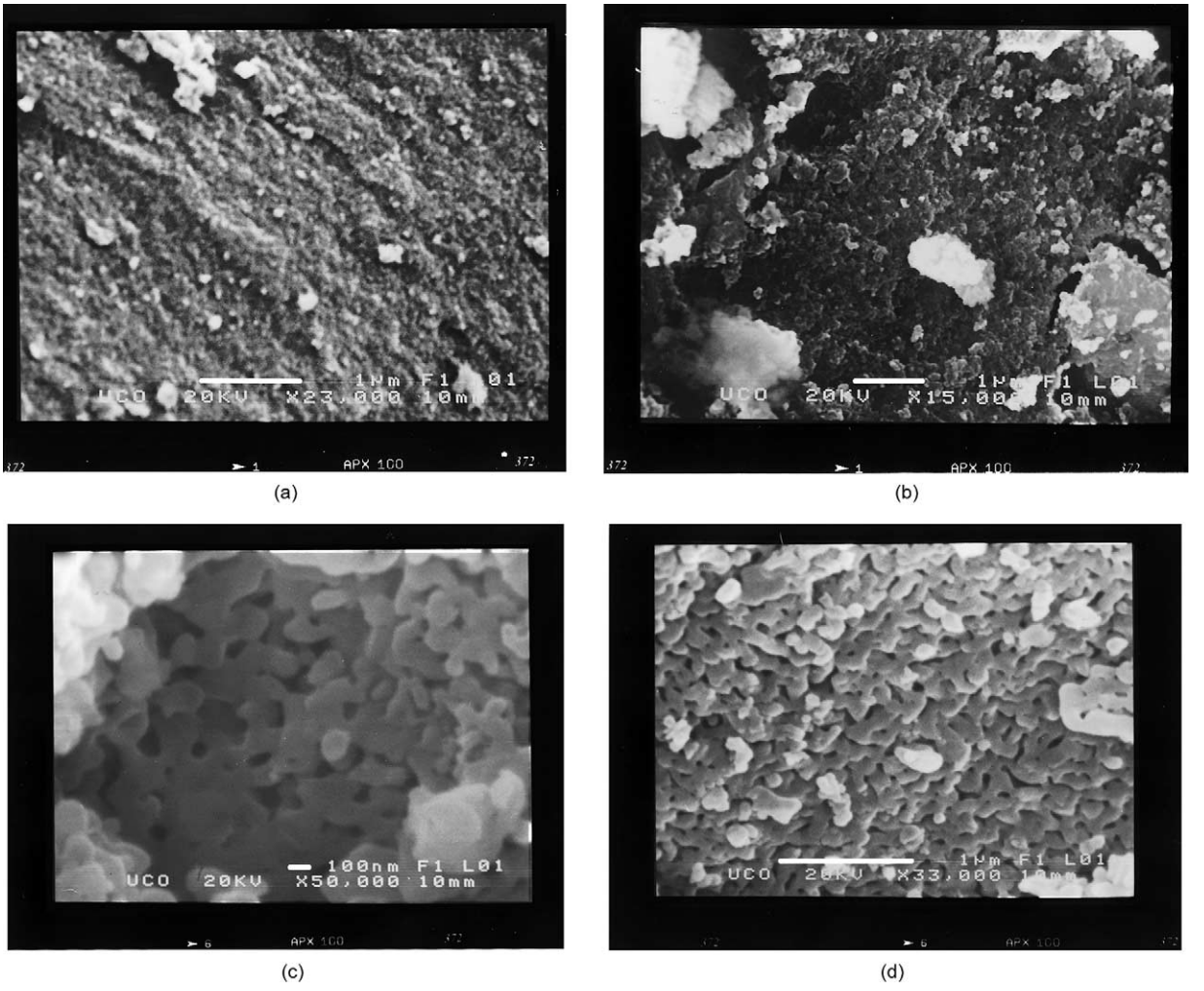

Fig. 7. Typical scanning electron micrographs for the studied solids: (a) calcined mAlPO-2; (b) mMgPO-1; (c) calcined mMgPO-1; (d) calcined mMgPO-2.

porous materials consisting of agglomerates (or to solids composed of orderly spheres of uniform size) exhibiting a narrow pore size distribution. Type H_2 cycles result from pores similar to those yielding H_1 type cycles but less uniform as regards cavity size distribution.

Solids mMgPO-1 and mMgPO-2 also possess higher specific surface areas than those obtained by precipitation from a solution, viz. 13 and 16 $m^2\,g^{-1}$, respectively, versus only about 6 $m^2\,g^{-1}$ [25]. Both solids exhibit a hysteresis cycle of the H_1 type.

3.6. Catalytic activity

The materials synthesized in this work were tested as catalysts for the transformation of isopropyl alcohol, which in this case undergoes two types of competitive reactions: intramolecular dehydration to propene and dehydrogenation to acetone. Both the magnesium phosphates and the aluminium phosphates were compared with a reference solid that was prepared by precipitation from a solution.

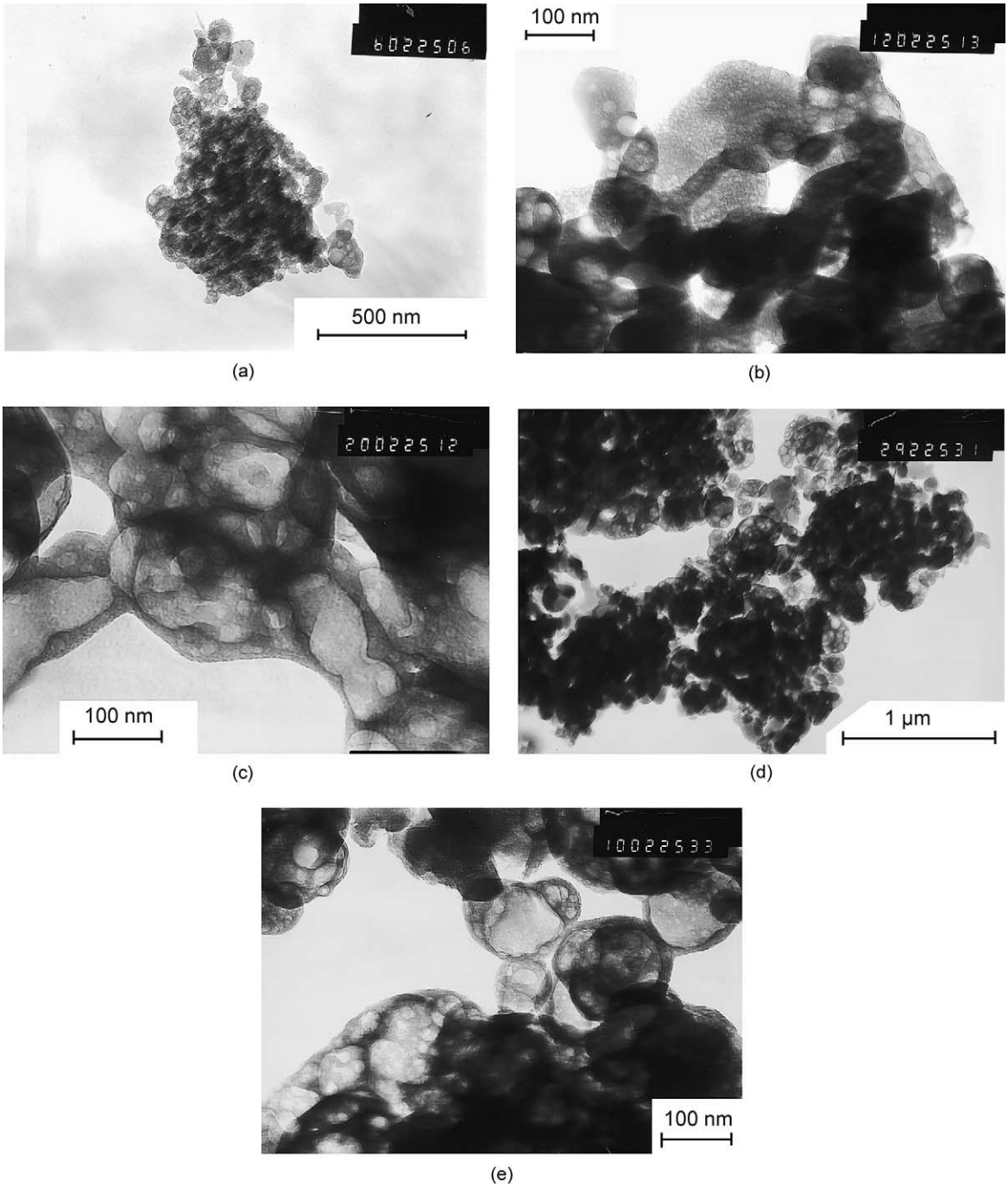

Fig. 8. Transmission electron micrographs for the studied solids: (a) mMgPO-1; (b) and (c) calcined mMgPO-1; (d) and (e) calcined mMgPO-2.

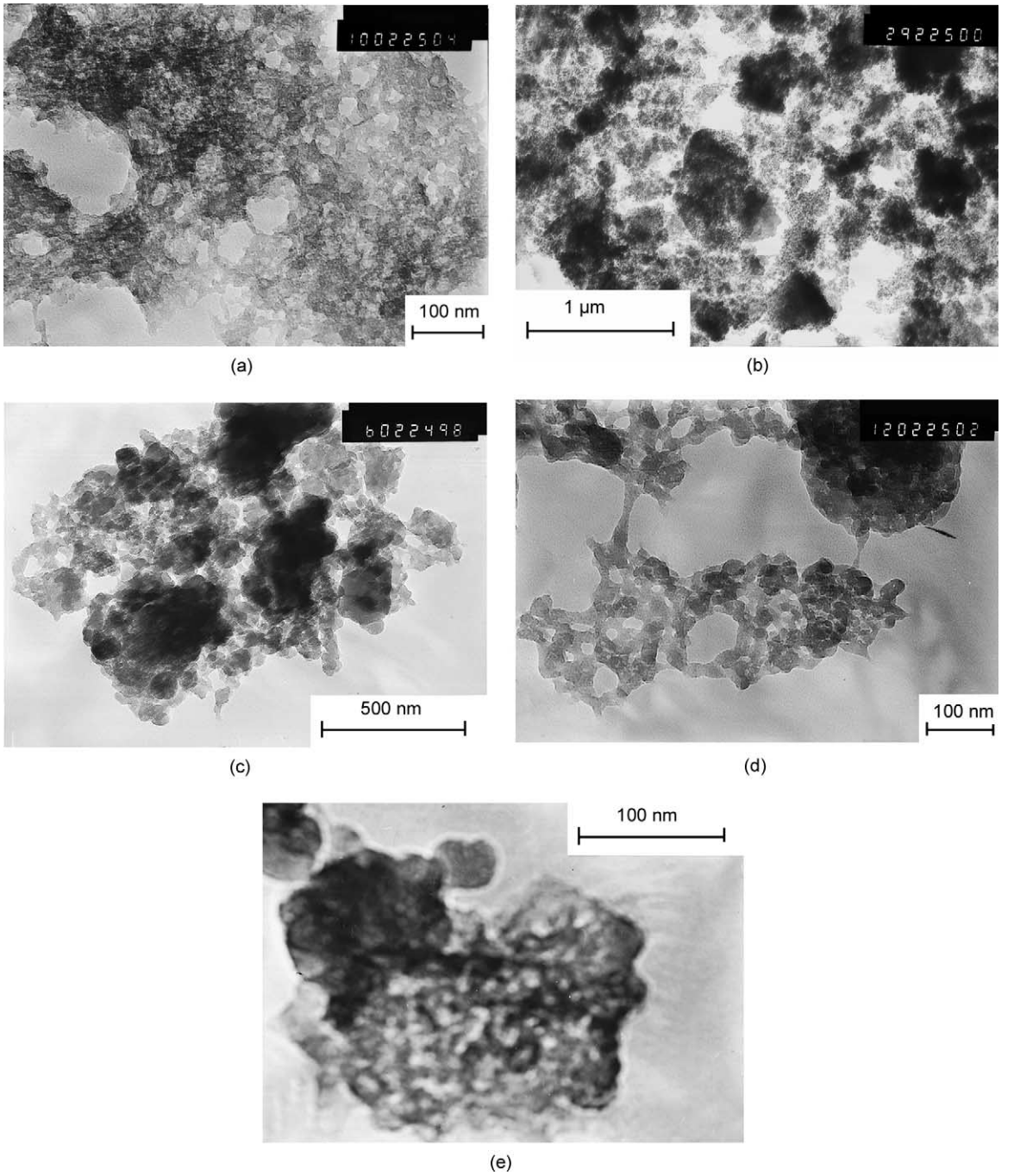

Fig. 9. Transmission electron micrographs for the studied solids: (a) mAlPO-1; (b–d) calcined mAlPO-1; (e) calcined mAlPO-2.

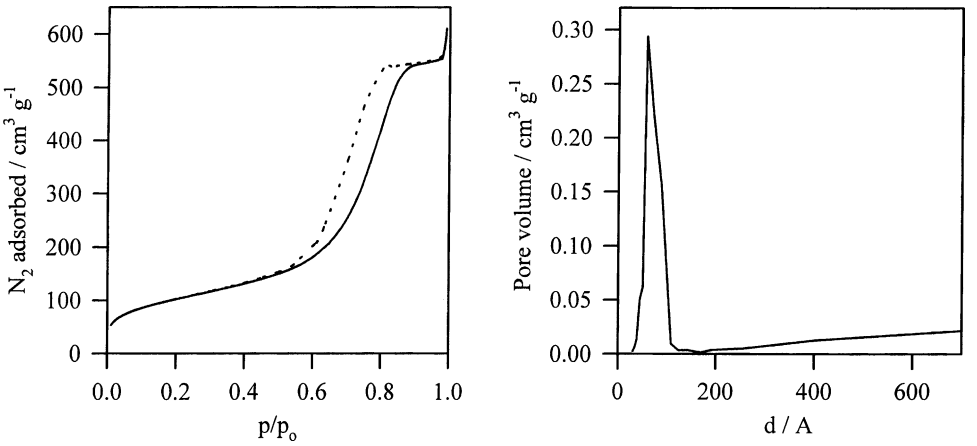

Fig. 10. N_2 isotherm showing the adsorption (solid line) and desorption (dotted line) branches (left) and pore size distribution (right) for solid mAlPO-2 calcined at 600 °C.

Fig. 11 shows the catalytic activity results for solids mMgPO-1 and mMgPO-2 following calcining, and that for the reference solid MgP-N ($S_{BET} = 6\,m^2\,g^{-1}$), which was obtained by precipitation of a solution containing magnesium nitrate and phosphoric acid with sodium hydroxide [25]. As expected from the characterization results, the solids obtained from microemulsions are structurally similar to those prepared from a solution; the reaction only yields the dehydration product (propene) and, especially, the dehydrogenation product (acetone). The surface chemical properties of the solids and their catalytic performance are closely related. The decomposition of alcohols is a model process for examining the acid–base properties of catalysts. Some authors ascribe the dehydrating ability of a solid to its surface acidity [34] and its dehydrogenating ability to its basicity [35]; others, however, believe that dehydrogenation is caused by both acid and basic sites via a concerted mechanism [36]. Consequently, our solids can all be considered essentially basic as regards catalytic behaviour. As can be seen from the results, the initial activity of the solids prepared from microemulsions exceeded that of the reference solid, MgP-N; however, after a long enough reaction time, solids mMgPO-1 and MgP-N were similarly active—and much less so than solid mMgPO-2 in any case. The initial activity of these solids was recovered upon heating at 600 °C; the conversion versus time curve was similar, so their deactivation was seemingly the result of reversible poisoning through adsorption of reagents and/or products.

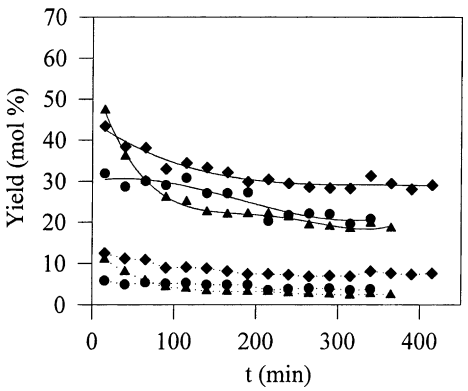

Fig. 11. Variation of the acetone (solid lines) and propene yield (dotted lines) with the reaction time in the transformation of isopropyl alcohol on solids: (•) MgP-N; (▲) mMgPO-1; (◆) mMgPO-2. Reaction conditions: N_2 flow-rate 30 ml min^{-1}, catalyst weight 0.100 g, feed rate 5.4 ml h^{-1}, $T = 500$ °C.

Solids mAlPO-1 and mAlPO-2 were compared with $AlPO_4$-F ($S_{BET} = 109\,m^2\,g^{-1}$), which was prepared by gelling of a solution with ammonium hydroxide. The sole reaction product obtained in the presence of these catalysts was propene, so the solids can be assumed to be essentially acid. Solids mAlPO-2 and $AlPO_4$-F exhibited similar activity that was much lower than that of mAlPO-1 in any case (Fig. 12).

The catalytic results provided by materials obtained from microemulsions are quite promising. No

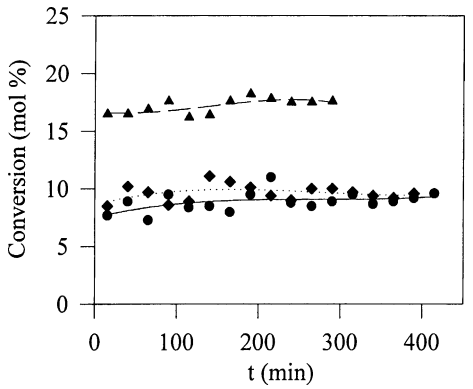

Fig. 12. Variation of the overall conversion with the reaction time in the transformation of isopropyl alcohol on solids: (•) $AlPO_4$-F; (▲) mAlPO-1; (◆) mAlPO-2. Reaction conditions: N_2 flow-rate 30 ml min^{-1}, catalyst weight 0.080 g, feed rate 5.4 ml h^{-1}, $T = 350\,^{\circ}C$.

clear-cut relationship between their textural properties and catalytic activity can still be established, however. In fact, their activity appears to depend, not on their surface area, but rather on the number of active sites available for a given reaction, which in turn depends on the number of structural defects present in the solid and on its surface structure. Thus, the slight difference in Al/P ratio and the presence of a higher initial content in octahedral aluminium in mAlPO-1 may be the result of an increased number of P–OH groups in this solid, which may account for its increased catalytic activity.

4. Conclusions

A procedure based on the use of reversed microemulsions was used to prepare various magnesium and aluminium orthophosphates that were found to be structurally and compositionally similar to solids obtained by precipitation from aqueous solutions. Specially prominent among the features of the new solids are their high specific surface area and a model pore size distribution (particularly in the aluminium phosphates). The solids were tested as catalysts in the model reaction involving the dehydration–dehydrogenation of isopropyl alcohol, where the magnesium phosphates exhibited a high selectivity towards acetone and the aluminium phosphates towards propene. The catalytic activity of these solids is similar to that of solids obtained by precipitation from aqueous solutions. In some cases, the solids prepared from microemulsions were even more catalytically active than their counterparts.

Acknowledgements

The authors would like to thank Spain's Dirección General de Investigación, Ministerio de Ciencia y Technología, for funding this research within the framework of Project BQU2001-2605 and Junta de Andalucía for additional financial support.

References

[1] H. Kessler, in: J.-M. Lehn (Ed.), Comprehensive Supramolecular Chemistry, Vol. 10, Pergamon, Oxford, 1996.; G. Alberti, T. Bein (Eds.), Solid-state Supramolecular Chemistry: Two- and Three-dimensional Inorganic Networks, Pergamon, Oxford, 1996, p. 425.
[2] C.T. Kresge, M.E. Leonowicz, W.J. Roth, J.C. Vartuli, J.S. Beck, Nature 359 (1992) 710.
[3] V. Pillai, P. Kumar, M.J. Hou, P. Ayyub, D.O. Shah, Adv. Colloid Interf. Sci. 55 (1995) 241.
[4] M. Boutonnet, J. Kizling, P. Stenius, G. Maire, Colloids Surf. 5 (1982) 209.
[5] J. Schmidt, C. Guesdon, R. Schomäcker, J. Nanoparticle Res. 1 (1999) 267.
[6] T. Hanaoka, W. Y. Kim, M. Kishida, H. Nagata, K. Wakabayashi, Chem. Lett. (1997) 645.
[7] M. Kishida, T. Fujita, K. Umakoshi, J. Ishiyama, H. Nagata, K. Wakabayashi, J. Chem. Soc., Chem. Commun. (1995) 763.
[8] W.-Y. Kim, H. Hayashi, M. Kishida, H. Nagata, K. Wakabayashi, Appl. Catal. A 169 (1998) 157.
[9] T. Masui, K. Fujiwara, Y. Peng, K. Machida, G. Adachi, Chem. Lett. (1997) 1285.
[10] J.B. Moffat, Catal. Rev. Sci. Eng. 18 (1978) 199.
[11] J.B. Moffat, in: M. Grayson, E.J. Griffith (Eds.), Topics in Phosphorus Chemistry, Vol. 10, Wiley, New York, 1980, p. 285.
[12] M.A. Aramendía, V. Borau, C. Jiménez, J.M. Marinas, F.J. Romero, J.A. Navío, J. Barrios, J. Catal. 157 (1995) 97.
[13] M.A. Aramendía, V. Borau, C. Jiménez, J.M. Marinas, F.J. Romero, Catal. Lett. 58 (1999) 53.
[14] M.A. Aramendía, V. Borau, C. Jiménez, J.M. Marinas, F.J. Romero, J. Catal. 183 (1999) 119.
[15] M.A. Aramendía, V. Borau, C. Jiménez, J.M. Marinas, F.J. Romero, Appl. Catal. A 183 (1999) 73.
[16] S. Sugiyama, K. Satomi, N. Kondo, N. Shigemoto, H. Hayashi, J.B. Moffat, J. Mol. Catal. 93 (1994) 53.
[17] S. Sugiyama, N. Kondo, K. Satomi, H. Hayashi, J.B. Moffat, J. Mol. Catal. A 95 (1995) 35.

[18] J.M. Campelo, A. García, J.F. Herencia, D. Luna, J.M. Marinas, A.A. Romero, J. Catal. 151 (1995) 307.
[19] A. Blanco, J.M. Campelo, A. García, D. Luna, J.M. Marinas, A.A. Romero, J. Catal. 137 (1992) 51.
[20] J.A. Cabello, J.M. Campelo, A. García, D. Luna, J.M. Marinas, J. Org. Chem. 49 (1984) 5195.
[21] C. Jiménez, J.M. Marinas, R. Perez-Ossorio, J.V. Sinisterra, An. Quím. 70 (1974) 860.
[22] R.M. Koros, E.J. Novak, Chem. Eng. Sci. 22 (1967) 470.
[23] J.M. Campelo, J.M. Marinas, S. Mendioroz, J.A. Pajares, J. Catal. 101 (1986) 484.
[24] T.T.P. Cheung, K.W. Willcox, M.P. McDaniel, M.M. Johnson, C. Bronnimann, J. Frye, J. Catal. 102 (1986) 10.
[25] M.A. Aramendía, V. Borau, C. Jiménez, J.M. Marinas, F.J. Romero, F.J. Urbano, J. Mol. Catal. A, 182–183 (2002) 25–34.
[26] M.A. Aramendía, V. Borau, C. Jiménez, J.M. Marinas, F.J. Romero, J. Colloid Interf. Sci. 219 (1999) 201.
[27] J. Sanz, J.M. Campelo, J.M. Marinas, J. Catal. 130 (1991) 642.
[28] M.A. Aramendía, V. Borau, C. Jiménez, J.M. Marinas, F.J. Romero, J.R. Ruiz, J. Solid State Chem. 135 (1998) 96.
[29] M.A. Aramendía, V. Borau, C. Jiménez, J.M. Marinas, F.J. Romero, F.J. Urbano, J. Colloid Interf. Sci. 240 (2001) 237.
[30] S. Brunauer, L.S. Deming, W.S. Deming, E. Teller, J. Am. Chem. Soc. 62 (1940) 1723.
[31] B. Rebenstorf, T. Lindblad, S.L.T. Andersson, J. Catal. 128 (1991) 293.
[32] K.S.W. Sing, D.H. Everest, R.A.W. Haul, L. Moscou, R.A. Pierotti, J. Rouquérol, T. Siemieniewska, Pure Appl. Chem. 57 (1985) 603.
[33] J.M. Thomas, W.J. Thomas, Principles and Practice of Heterogeneous Catalysis, VCH, Weinheim, 1997, p. 276.
[34] F. Figueras-Rocca, L. Mourgues, Y. Trambouze, J. Catal. 14 (1969) 107.
[35] Y. Matsumura, K. Hashimoto, S. Yoshida, J. Catal. 117 (1989) 135.
[36] A. Gervasini, A. Auroux, J. Catal. 131 (1991) 190.